

## Mechanochemical Synthesis of High Crystalline Cerium Hexaboride Nanoparticles from CeO<sub>2</sub>-B<sub>2</sub>O<sub>3</sub>-Mg Ternary System

Omid Torabi,<sup>a</sup> Sanaz Naghibi,<sup>b\*</sup> Mohammad-Hossein Golabgir<sup>a</sup> and Amin Jamshidi<sup>a</sup><sup>a</sup>Young Researchers and Elite Club, Najafabad Branch, Islamic Azad University, Najafabad, Iran<sup>b</sup>Young Researchers and Elite Club, Shahreza Branch, Islamic Azad University, Shahreza, Iran

(Received: Nov. 25, 2015; Accepted: Feb. 23, 2016; Published Online: Apr. 5, 2016; DOI: 10.1002/jccs.201500479)

High crystalline cerium hexaboride (CeB<sub>6</sub>) nanoparticles (NPs) were synthesized using mixture of magnesium (Mg), cerium oxide (CeO<sub>2</sub>) and boron oxide (B<sub>2</sub>O<sub>3</sub>) via the mechanochemical process at room temperature. Based on the results, magnesiothermic reduction of B<sub>2</sub>O<sub>3</sub> occurred after about 2 h of milling in a mechanically induced self-sustaining reaction (MSR). The significant amount of heat produced by the reduction reaction resulted in CeO<sub>2</sub> reduction to elemental Ce which finally reacted with elemental B and formed CeB<sub>6</sub> compound. According to XRD analyses, the degree of crystallinity and lattice parameter of the product was calculated about 93% and 4.1458 Å, respectively. The morphology observations revealed that the synthesized CeB<sub>6</sub> had semi-cubic shape with the range of size 25–60 nm. The synthesis of CeB<sub>6</sub> during the thermal treatment was studied by simultaneous thermal analysis (STA) technique. It was found that the reduction of B<sub>2</sub>O<sub>3</sub> took place after melting of Mg meanwhile, no CeB<sub>6</sub> phase achieved even up to 1100 °C.

**Keywords:** Mechanochemistry; Cerium hexaboride; Formation mechanism; XRD; TEM.

### INTRODUCTION

CeB<sub>6</sub> is an engineering ceramic with excellent electronic and magnetic characteristics, such as high thermal stability, low volatility, low work function (2.5 eV), high stability in vacuum and high melting point (> 2000 °C). It owns one of the highest electron emissivity which has been found to use in high-tech equipment such as cathodes for electron microscopy, high current applications in microwave tubes, electron-beam welders, X-ray sources and etc.<sup>1</sup>

Various techniques have been reported to prepare CeB<sub>6</sub>. The two conventional methods for synthesizing CeB<sub>6</sub> are (i) direct reaction of B and Ce at an elevated temperature and (ii) carbothermal reduction of CeO<sub>2</sub>-B<sub>2</sub>O<sub>3</sub> mixture.<sup>2</sup> These methods require high temperature and lead to produce a powder with low purity and poor sinterability;<sup>3</sup> therefore, it is important to develop the methods to achieve high-quality products.

Sahadev *et al.* have synthesized CeB<sub>6</sub> single crystals by the floating zone route.<sup>4</sup> CeB<sub>6</sub> thin film was prepared by using a molecular beam epitaxy (MBE) method.<sup>5</sup> Kushkhov *et al.* used electroreduction of Ce ions with fluoroborate ions to prepare CeB<sub>6</sub> nanotube.<sup>6</sup> The high cost of the equipment needed, is the main disadvantage of these techniques which limits its applicability.<sup>7</sup>

In this regard, Dou *et al.* prepared CeB<sub>6</sub> nanopowder by high-temperature self-propagating synthesis (SHS) method. They milled the powder mixture (including CeO<sub>2</sub>, B<sub>2</sub>O<sub>3</sub>, Mg and KClO<sub>3</sub>) for 12 h and then pressed and placed in a combustion chamber. Their results showed that the single phase CeB<sub>6</sub> powder with particle size of less than 150 nm was achieved by the SHS method.<sup>3</sup> Due to the general restrictions in thermal techniques such as high required temperature, non-uniform phase, large particle size and so on, the main aim of this work was to find an effective technique to prepare CeB<sub>6</sub> NPs with high purity and high degree of crystallinity.

Mechanochemistry is the simultaneous mechanical and chemical reactions in a molecular scale; including mechanical breakage and chemical reactions. This is an in-situ solid-state method in which the starting powders mixture reacts at room temperature or at least much lower temperature. This phenomenon is related to the mechanical breakage and cold deformation of the particles during high energy milling. This method may decrease reaction time, save energy and produce high purity of products;<sup>8</sup> therefore, the mechanochemical is a promising approach for the synthesis of advanced materials processing such as carbides,<sup>9–10</sup> nitrides,<sup>11–12</sup> intermetallics<sup>13</sup> and borides.<sup>14</sup> This method has been applied to synthesize TiB<sub>2</sub>,<sup>14</sup> NbC-NbB<sub>2</sub>,<sup>15</sup> CrB<sub>2</sub>,<sup>16</sup>

\* Corresponding author. Tel: +98 31 53292060; Fax: +98 31 53502701; Email: naghibi@iaush.ac.ir

Mo<sub>2</sub>B,<sup>17</sup> Al<sub>2</sub>O<sub>3</sub>-BN<sup>18</sup> by this research team. During the milling process, the exothermic reduction of the metal oxides by Al or Mg releases large amount of heat and then, the generated elemental metals react with B and/or C to synthesize borides and/or carbides.<sup>14-18</sup>

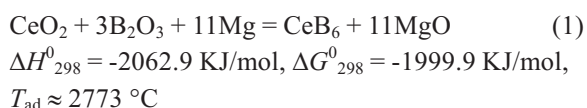
Akgun *et al.* have been prepared CeB<sub>6</sub> by mechanochemical method. The powder mixture (including CeO<sub>2</sub>, B<sub>2</sub>O<sub>3</sub> and Mg) was milled for long time of 30 h. The obtained powder was a mono-phase CeB<sub>6</sub> with the particle size of about 240 nm.<sup>7</sup> It is well determined<sup>8</sup> that the level of contamination significantly increases if the as-received powder mixture is milled for long times, hence, it is advantageous that the products would be obtained in short durations.

The purpose of this research is to investigate the formation of CeB<sub>6</sub> NPs by using CeO<sub>2</sub>, Mg and B<sub>2</sub>O<sub>3</sub> during the high energy ball mill. Fundamental aspects of reaction path in CeO<sub>2</sub>-B<sub>2</sub>O<sub>3</sub>-Mg ternary system as well as the influences of B<sub>2</sub>O<sub>3</sub> content were studied. Afterward, the system will be described in view point of thermodynamic and thermal treatment.

## RESULTS AND DISCUSSION

### Mechanochemistry of Mg/CeO<sub>2</sub>/B<sub>2</sub>O<sub>3</sub> system

The theoretical chemical reaction taking place during the synthesis of CeB<sub>6</sub> in CeO<sub>2</sub>-B<sub>2</sub>O<sub>3</sub>-Mg system can be described by Eq. (1).



According to the theoretical thermodynamic calculations, the reaction of stoichiometric amount of starting materials is highly exothermic and favorable at room temperature. The adiabatic temperature of Eq. (1) met the critical value of 1800 K, suggesting the reaction type is MSR. In this type of reactions, the minimum amount of energy is needed to start a self-propagating combustion reaction. The activation energy is provided by the milling of mixture, then the combustion reactions occur and the vessel temperature increases.<sup>8</sup>

The XRD patterns of the stoichiometric powder mixture milled for 1.5, 2 and 4 h are shown in Figure 1. The XRD pattern of the sample after 1.5 h of milling illustrates that no considerable phase changes occurred. The peaks of B<sub>2</sub>O<sub>3</sub> disappeared due to the transformation from crystal

state into its amorphous.<sup>19</sup> In this case, only the main peaks of Mg [JCPDS: 35-821] and CeO<sub>2</sub> [JCPDS: 75-390] were observed. The sharp peaks of products (CeB<sub>6</sub> and MgO) were clearly observed in the sample milled for 2 h. The abrupt phase transformation in the XRD pattern and the calculated T<sub>ad</sub> (~2773 °C) reveals that the type of reaction in the stoichiometric mixture of Mg-B<sub>2</sub>O<sub>3</sub>-CeO<sub>2</sub> was MSR. A loud voice of explosive reactions which was recognized after 2 h of milling confirms this fact. As can be seen, a negligible trace of CeO<sub>2</sub> was still remained. This can be explained by following reasons: (i) the accumulation of starting materials in the dead regions of the milling pot and (ii) the insufficient mixing of the reactants at short time. The presence of negligible unreacted materials after the ignition is a typical characteristic of MSR type of reactions.<sup>20</sup>

By prolonging the milling time for another 2 h (4 h), the unreacted powders were exposed to the ball hits and high temperature, thus the required energy for completion of reactions was supplied and the remaining trace of CeO<sub>2</sub> was removed from the XRD pattern. It must be noted that, the explosion did not occur in this step, because the amount of unreacted powder was negligible and hence the heat released by reactions were not as high as enough to explode.

By comparing the intensities of CeB<sub>6</sub> and MgO peaks after 2 and 4 h of milling, it can be concluded that increasing the milling time slightly decreases the height of XRD peaks, due to plastic deformation, particle size reduction and amorphization.

Figure 2 shows the phase component of sample milled for 4 h after leaching. As can be observed, the charac-

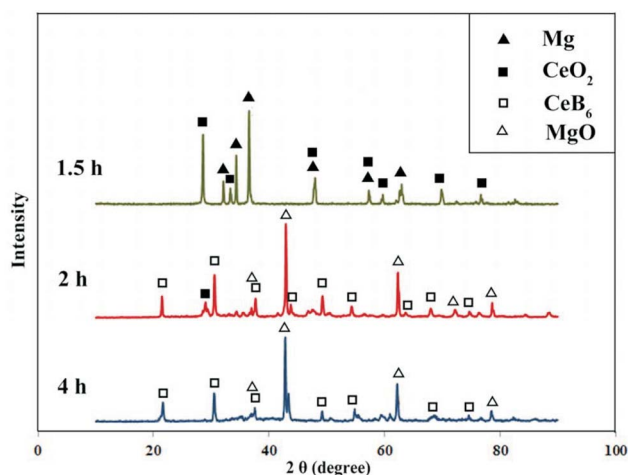


Fig. 1. XRD patterns of the stoichiometric powder mixture after 1.5, 2 and 4 h of milling.

teristics traces of MgO are completely removed and CeB<sub>6</sub> [JCPDS No. 38-1455] appears as a unique phase. Miller indexes are provided for the cubic CeB<sub>6</sub> with a space group of *Pm3m*. The standard lattice parameter is 4.1412 Å, whereas the estimated value data from the XRD analysis is 4.1458 Å. This deviation can be related to the strain, defects and chemical compound.<sup>21</sup> The less deviation is measured, the higher quality of crystals is achieved. Degree of crystallinity of the prepared CeB<sub>6</sub> was calculated about 93%. In addition, the allocated score of profile fitting via the search/match software (PANalytical X'Pert HighScore) was 95%. Therefore, according to (i) tiny difference between the standard and calculated lattice parameter values, (ii) the high degree of crystallinity and (iii) high score of profile fitting, it can be concluded that this method can be a very effective technique to synthesize high-crystalline and high-quality CeB<sub>6</sub> NPs.

Figure 3 shows TEM micrographs of the as-synthesized NPs before and after leaching process. According to Figure 3-A, the un-leached powder contains some semi-spherical particles in the range of 10–20 nm as well as some semi-cubic particles in the range of 30–60 nm. Figure 3-B shows only semi-cubic particles with particle size of 25–60 nm in the leached sample. By comparing these Figures (Figures 3-A and B), it can be concluded that semi-spherical MgO NPs were removed via leaching. On the other hand, in accordance to XRD result (Figure 2) and TEM image (Figure 3-B), the phase component of the semi-cubic particles is CeB<sub>6</sub>. It can be seen that these NPs have curved

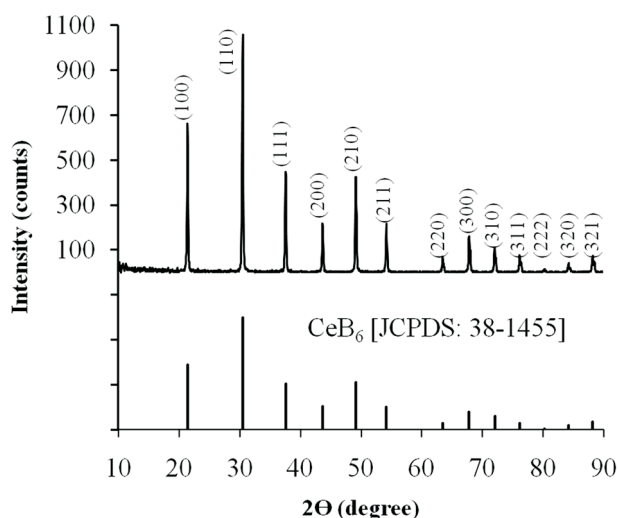


Fig. 2. XRD pattern of the 4 h milled sample after the leaching process.

corners. This phenomenon can be explained by the mechanical damage during milling process.

The SEM micrographs of the as-synthesized CeB<sub>6</sub> NPs are illustrated in Figure 4. The powder agglomeration can be seen before and after the leaching. The agglomeration is an inevitable phenomenon in the preparation of NPs via mechanochemical systems due to the higher specific surface area.

#### The sequence and mechanism of chemical reactions

The mechanism for the preparation of CeB<sub>6</sub> in the stoichiometric mixture of Mg-B<sub>2</sub>O<sub>3</sub>-CeO<sub>2</sub> can be explained as follows.



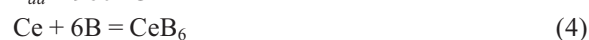
$$\Delta H_{298}^0 = -531.3 \text{ KJ/mol}, \Delta G_{298}^0 = -513.5 \text{ KJ/mol},$$

$$T_{ad} \approx 2240 \text{ }^\circ\text{C}$$



$$\Delta H_{298}^0 = -112.8 \text{ KJ/mol}, \Delta G_{298}^0 = -111.6 \text{ KJ/mol},$$

$$T_{ad} \approx 960 \text{ }^\circ\text{C}$$



$$\Delta H_{298}^0 = -351.5 \text{ KJ/mol}, \Delta G_{298}^0 = -342.3 \text{ KJ/mol},$$

$$T_{ad} \approx 3701 \text{ }^\circ\text{C}$$

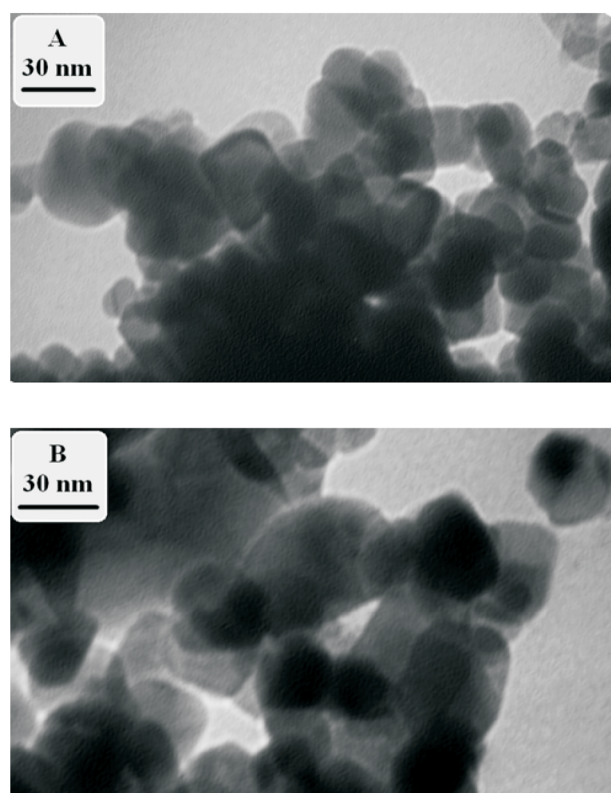


Fig. 3. TEM micrographs of the as-synthesized NPs. (A) un-leached sample, (B) leached sample.

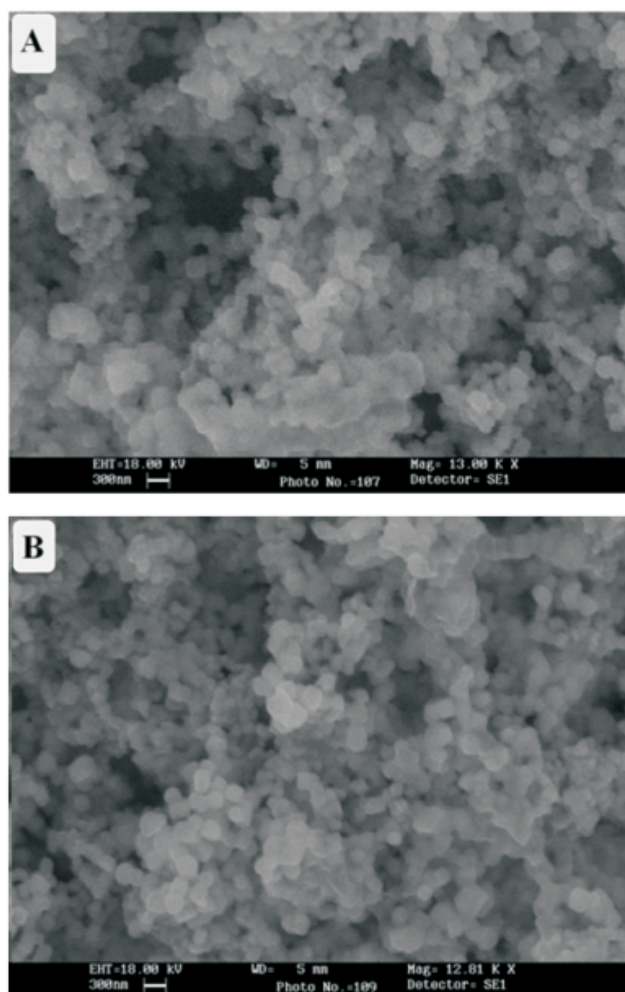
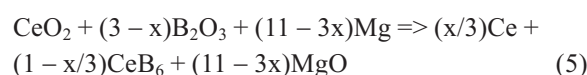


Fig. 4. SEM micrographs of the as-synthesized NPs. (A) un-leached sample, (B) leached sample.

By considering thermodynamic evaluations, it can be predicted that, in the presence of Mg, B<sub>2</sub>O<sub>3</sub> and CeO<sub>2</sub>, magnesium initially reduces B<sub>2</sub>O<sub>3</sub> (due to higher negative values of  $\Delta G^0$  and  $\Delta H^0$ ) in MSR manner (Eq. 2) and produces boron as well as significant amount of heat. This heat can provide enough energy to active magnesiothermic reduction of CeO<sub>2</sub> to form elemental Ce (Eq. 3). Consequently, CeB<sub>6</sub> can be synthesized by reaction between the generated B and Ce during a high exothermic reaction (Eq. 4). It worth mentioning that all these reactions occurred at the same time; therefore, the only the peaks of MgO and CeB<sub>6</sub> was observed in XRD pattern of sample just after explosion. The presence of remaining CeO<sub>2</sub> peaks (see Figure 1) confirmed the suggested reaction mechanism. Regarding the calculated adiabatic temperatures, the Eq. (2) and (4) can be considered as the MSR type, whereas the reduc-

tion of CeO<sub>2</sub> (Eq. 3) is a progressive reaction.

In order to further evaluate the proposed mechanism and to identify the effect of B<sub>2</sub>O<sub>3</sub> content on the boride formation phenomena, the value of B<sub>2</sub>O<sub>3</sub> in the B<sub>2</sub>O<sub>3</sub>-CeO<sub>2</sub>-Mg mixture was changed according to the following general reaction:



When  $x = 0$ , the stoichiometric portion of the reactants was achieved. The XRD pattern of the leached sample milled for 4 h was shown in Figure 5-a, approving the formation of CeB<sub>6</sub> as a unique phase. When  $x = 1$ , the B<sub>2</sub>O<sub>3</sub> content decreased about 10%, which means that the released energy from the reduction of B<sub>2</sub>O<sub>3</sub> decreased, which affected the reduction of CeO<sub>2</sub>. In this reason, the traces of CeO<sub>2</sub> were reminded in XRD pattern of this sample (Figure 5-b). Further decrease in the B<sub>2</sub>O<sub>3</sub> content ( $x = 2$ ) resulted in more decrease in CeB<sub>6</sub> peaks intensities and more increase in the remaining CeO<sub>2</sub> peaks height (Figure 5-c). In other words, in non-stoichiometric conditions, the B<sub>2</sub>O<sub>3</sub> content is not as high enough to provide required energy via reduction reaction to complete the Eq. (4). It seems that when  $x$  is equal to two, the amount of synthesized CeB<sub>6</sub> decreased rigorously, due to the insufficient heat generated to overcome barrier energy.

#### Thermal analysis

STA analysis was utilized to investigate the reaction sequence of this system during heat treatment (Figure 6). As can be seen, there are three endothermic peaks (at 120, 170 and 645 °C) and an exothermic event at 707 °C. The

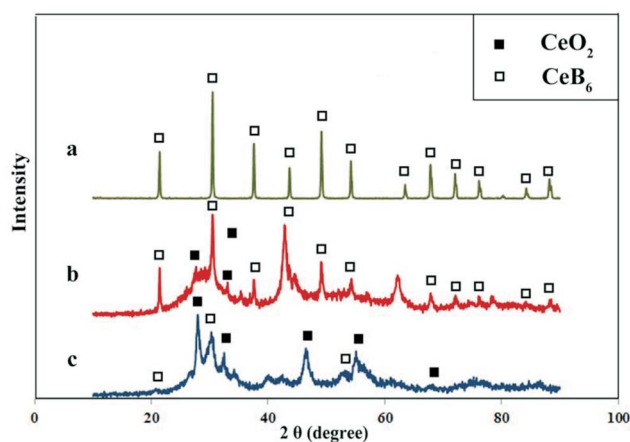


Fig. 5. XRD patterns of samples a ( $x = 0$ ), b ( $x = 1$ ) and c ( $x = 2$ ) after 4 h of milling.

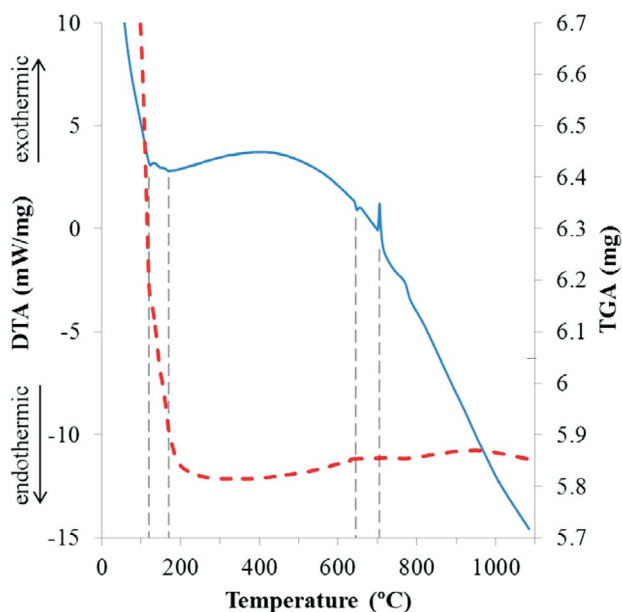


Fig. 6. STA curve of the as-blended mixture of the CeO<sub>2</sub>-B<sub>2</sub>O<sub>3</sub>-Mg system.

first weak endotherm, corresponding to the decrease region in the TG curve, is ascribed to vaporization of the water absorbed to boron oxide. Usually B<sub>2</sub>O<sub>3</sub> particles adsorb water on their surfaces and lose it during heating. There is a peak at about 650 °C in STA curve, which can be related to the melting of Mg. The exothermic peaks at approximately 700 °C without any weight changing can be ascribed to the initiation of the magnesiothermic reaction of boron oxide as predicted in thermodynamic calculations. This temperature is too low for the reduction of CeO<sub>2</sub>.<sup>22</sup> Low intensity of this peak indicates that this reaction didn't occur completely. On the other hand, increasing the temperature to 1100 °C had no effect on DTA curve. This means that the reduction of CeO<sub>2</sub> by Mg needs higher temperature.

Based on the thermal analysis, melting of Mg and lack of the required energy for reduction of CeO<sub>2</sub> are obstacles of SHS reaction. It seems that CeB<sub>6</sub> production from CeO<sub>2</sub> is not possible via direct heating. The similar results were reported by Jalaly et al in the Mg/ZrO<sub>2</sub>/B<sub>2</sub>O<sub>3</sub> system.<sup>22</sup>

## EXPERIMENTAL

For synthesis of CeB<sub>6</sub>, the stoichiometric amounts of cerium oxide (CeO<sub>2</sub>: Merck Co., > 99%, ~3 μm), magnesium (Mg: Merck Co., 99.7%, 40 ± 5 μm) and boron oxide (B<sub>2</sub>O<sub>3</sub>: Merck Co., 99.9%, 30 ± 5 μm) were mixed.

Powder blends were milled in a planetary mill at 500 rpm with hardened carbon steel balls (Φ = 10 mm, n = 5) in a hardened

chromium steel container with a balls-to-powder ratio of 20. To prevent oxidation, the milling pots were filled with high-purity argon gas and the mill was stopped and allowed to cool for 15 min after each 1 h of grinding.

For removing the produced by-products such as MgO, the powder after milling was leached with 18% hydrochloric acid (HCl) for 1 h. The solution was filtered and the purified products were repeatedly washed by distilled water to eliminate extra HCl until the pH value reached a value of about 7. The residue on the filter was dried at 90 °C for 2 h.

The thermodynamic studies were conducted base on thermodynamic data ( $\Delta H_{298}^0$ ,  $\Delta G_{298}^0$  and  $T_{ad}$ ) that were collected from Kubaschewski's book.<sup>23</sup>

The thermal behavior of this system was characterized by means of simultaneous thermal analysis (STA) in an instrument (BAHR THERMOARALYSE, 503, Germany). 50 mg of the powder mixture was weighted and held in an alumina crucible and heated under argon flow at a heating rate of 10 °C·min<sup>-1</sup> up to 1100 °C.

The powder mixtures after milling and after leaching were characterized by XRD (D8 advance spectrometer, Bruker, Germany) with Cu radiation ( $K\alpha = 1.540598 \text{ \AA}$ ) and a Ni filter. The diffraction patterns were analyzed using PANalytical X'Pert HighScore software by comparison with the JCPDS database.

The degree of crystallinity of the NPs was quantitatively evaluated. In this method, 'sum of net area' / 'sum of total area' in PANalytical X'Pert High Score software was the criterion for the degrees of crystallinity. To calibrate the results, backgrounds of peaks were determined by considering 100% crystallinity for the commercial CeO<sub>2</sub>. This method has been reported elsewhere.<sup>24</sup>

As the CeB<sub>6</sub> is a cubic crystal, the relation between the interplanar d-spacing (d), miller indices (*h k l*) and lattice parameter is described by  $a^2 = d^2 / (h^2 + k^2 + l^2)$ . The interplanar d-spacing and miller indices are determined by XRD software for each peak; therefore, the lattice parameter could be achieved.<sup>21</sup>

The microstructures of the samples were observed by SEM (LEO, 435 VP, Germany, at 18 kV) and TEM (Philips CM200 FEG, Netherlands, at 200 kV).

## CONCLUSIONS

The mechanochemical method was successfully applied to synthesize high crystalline cerium boride nanopowder from a mixture of Mg-CeO<sub>2</sub>-B<sub>2</sub>O<sub>3</sub> at room temperature. As predicted by thermodynamic evaluations, the reaction mode in this system was MSR with an ignition time of 2 h. According to the experimental findings, at first, magnesium reduced B<sub>2</sub>O<sub>3</sub> in a self-sustaining manner and

produced elemental B and MgO as well as a significant amount of heat which promoted the reduction of CeO<sub>2</sub>. The B<sub>2</sub>O<sub>3</sub> content played an important role and the decrease in its value changed the mechanochemical behavior from MSR to progressive reaction. The morphology evaluations illustrated that after 4 h of milling, the CeB<sub>6</sub> NPs made large agglomerations and the range of particle size was lower than 100 nm. The degree of crystallinity and lattice parameter of synthesized cerium boride was calculated about 93% and 4.1458 Å, respectively. Investigation on the thermal treatment behavior supported the proposed reaction mechanism.

## REFERENCES

1. Bauer, E. *Surface Microscopy with Low Energy Electrons*; Springer-Verlag: New York, 2014.
2. Post, B.; Moskowitz, D.; Glaser, F. W. *J. Am. Chem. Soc.* **1956**, *78*, 1800.
3. Dou, Z.; Zhang, T.; Guo, Y.; He, J. *J. Rare Earths* **2012**, *30*, 1129.
4. Sahadev, N.; Biswas, D. N.; Thakur, S.; Ali, K.; Balakrishnan, G.; Maiti, K. *AIP Conf. Proc.* **2013**, 828.
5. Hatanaka, D.; Asanuma, E.; Takeda, K.; Ikeda, T.; Nakamura, M.; Nakanishi, Y.; Iga, F.; Harada, Y.; Yamaguchi, H.; Yoshizawa, M. *JPS Conf. Proc.* **2014**, *3*, 110491.
6. Kushkhov, H. B.; Vindizheva, M. K.; Mukozheva, R. A.; Abazova, A. H.; Tlenkopachev, M. R. *J. Mater. Sci. Chem. Eng.* **2014**, *2*, 57.
7. Akgun, B.; Sevinc, N.; Camurlu, H. E.; Topkaya, Y. *Int. J. Mater. Res.* **2013**, *104*, 403.
8. Balaz, P. *Mechanochemistry in Nanoscience and Minerals Engineering*; Springer-Verlag: Berlin, 2008.
9. Hoseinpur, A.; Vahdati-Khaki, J.; Sadat-Marashi, M. *Mater. Res. Bull.* **2013**, *48*, 399.
10. Khabbaz, S.; Honarbakhsh-Raouf, A.; Ataie, A.; Saghafi, M. *Int. J. Refract. Met. Hard Mater.* **2013**, *41*, 402.
11. Jacobsen, C. J. H.; Zhu, J. J.; Lindelov, H.; Jiang, J. Z. *J. Mater. Chem.* **2002**, *12*, 3113.
12. Roldan, M. A.; Lopez-Flores, V.; Alcala, M. D.; Ortega, A.; Real, C. J. *Eur. Ceram. Soc.* **2010**, *30*, 2099.
13. Blanco, V.; Esquivel, M. R. *Adv. Powder Technol.* **2013**, *24*, 86.
14. Torabi, O.; Golabgir, M. H.; Tajizadegan, H.; Naghibi, S.; Jamshidi, A. *J. Mater. Res.* **2014**, *105*, 778.
15. Torabi, O.; Naghibi, S.; Golabgir, M. H.; Tajizadegan, H.; Jamshidi, A. *Ceram. Int.* **2015**, *41*, 5362.
16. Torabi, O.; Golabgir, M. H.; Tajizadegan, H. *Int. J. Refract. Met. Hard Mater.* **2015**, *51*, 50.
17. Torabi, O.; Ebrahimi-Kahrizsangi, R.; Golabgir, M. H.; Tajizadegan, H.; Jamshidi, A. *Int. J. Refract. Met. Hard Mater.* **2015**, *48*, 102.
18. Nikkhah, A. J.; Torabi, O.; Ebrahimi-Kahrizsangi, R.; Naghibi, S.; Jamshidi, A. *Ceram. Int.* **2014**, *40*, 5559.
19. Yaghoubi, M.; Torabi, O. *Int. J. Refract. Met. Hard Mater.* **2014**, *43*, 132.
20. Takacs, L. *Prog. Mater. Sci.* **2002**, *47*, 355.
21. Ebrahimi-Kahrizsangi, R.; Alimardani, M.; Torabi, O. *Int. J. Refract. Met. Hard Mater.* **2015**, *52*, 90.
22. Jalaly, M.; Bafghi, M. S.; Tamizifar, M.; Gotor, F. J. *J. Alloy Compd.* **2014**, *588*, 36.
23. Kubaschewski, O.; Alcock, C. B. *Metallurgical thermochemistry*, 5<sup>th</sup> ed.; Pergamon Press: Oxford, UK, 1979.
24. Naghibi, S.; Faghihi Sani, M. A.; Madaah Hosseini, H. R. *Ceram. Int.* **2014**, *40*, 4193.